Curvature Orientation Histograms for Detection and Matching of Vascular Landmarks in Retinal Images

Keerthi Ram, Yogesh Babu and Jayanthi Sivaswamy

Centre for Visual Information Technology, IIIT-Hyderabad, India

ABSTRACT

Registration is a primary step in tracking pathological changes in medical images. Point-based registration requires a set of distinct, identifiable and comparable landmark points to be extracted from images. In this work, we illustrate a method for obtaining landmarks based on changes in a topographic descriptor of a retinal image. Building on the curvature primal sketch introduced by Asada and Brady[1] for describing interest points on planar curves, we extend the notion to grayscale images. We view an image as a topographic surface and propose to identify interest points on the surface using the surface curvature as a descriptor. This is illustrated by modeling retinal vessels as trenches and identifying landmarks as points where the trench behaviour changes, such as it splits or bends sharply. Based on this model, we present a method which uses the surface curvature to characterise landmark points on retinal vessels as points of high dispersion in the curvature orientation histogram computed around the points. This approach yields junction/crossover points of retinal vessels and provides a means to derive additional information about the type of junction. A scheme is developed for using such information and determining the correspondence between sets of landmarks from two images related by a rigid transformation. In this paper we present the details of the proposed approach and results of testing on images from public domain datasets. Results include comparison of landmark detection with two other methods, and results of correspondence derivation. Results show the approach to be successful and fast.

Keywords: Registration, Retinal Images, Landmarks

1. DESCRIPTION OF PURPOSE

Retinal images provide visual information to clinical experts on pathological changes, and early signs of systemic diseases like diabetes and hypertension. Changes in the retinal image over time are essential to observe and track in the diagnostic process. In automated analysis, a set of known image primitives (features) like points, lines and curves are used for finding the change/transformation. For instance in point-based registration, key points are extracted from the two images and the transformation is estimated using only the coordinates of the matched key points. Such key features are called landmarks. Landmarks are anatomically significant, visually salient, distinct features in the image that are identifiable and comparable across images. Apart from registration, landmarks are useful in several tasks including localization of disorders, surgery planning, constructing mosaics and synthesising panoramic views.

1.1 Background

Several previous work use the bifurcation points (junctions) and crossover points of vessels as landmarks.[2–4] This is because they are meaningful landmarks, at a semantically higher level than points, lines and curves on the image. Morphological processing using revolving structural elements of T-shape has been used to locate vessel bifurcation points, after reducing the vessels to 1-pixel wide paths.[3] Changes in image gradient information have also been used to select landmark points.[2] Here, an edge-direction dispersion measure is computed in a window W around every edge pixel and its local maximas are declared as landmark points. A fixed window W will result in inconsistencies in localisation of landmarks as well as their density along the tree, since the branches in the vessel tree of a retinal image are of varying thickness. Consequently, after additional processing like smoothing of histograms and pose clustering, only a subset of the landmarks are used to derive a set of

Further author information: (send correspondence to Keerthi Ram)
E-mail: keerthiram@research.iiit.ac.in

corresponding landmarks from a pair of images. Motivated by the need to extract the full vessel tree accurately, a recent approach uses a multiscale approach and matched filters to trace the medial axis of thick and very thin vessels.[4] Landmark points on this vessel tree are detected at intersections of multiple traces. However, the vessel extraction step is computationally quite complex.

In point-set based registration, the need is only for detection of a set of landmark points with maximal information content. Hence, an approach that does not require accurate vessel tree extraction is of interest. In this paper, we present such a method, which still guarantees the points to be located on vessel branching/crossover points and encapsulates additional information which is directly useful in matching landmarks across image pairs.

2. METHOD

Interest points have been described for planar curves, by mapping discontinuities in the curve to the local tangent-orientation space and obtaining descriptions from the new space.[1] The underlying hypothesis is that discontinuities have higher information content and are hence of interest. We propose a grayscale analogy and view a given image as a topographical surface S and examine how it changes to locate interesting points, specifically by analysing the way S *bends* at any point. Vessel branching points and crossovers are subsets of such points of significant bend in S.

Let us consider detecting landmarks from a given color fundus image I_c. We restrict our analysis to the green plane I_g of the image which has maximum contrast. We embed the grayscale image I_g in $3D$ where it can be viewed as a topographical surface S_I. The intrinsic surface curvature is a suitable descriptor of S_I, assuming I_g to be twice differentiable. The curvature descriptor consists of four quantities based on the Hessian matrix of I_g. These are two Eigen values a_1 and a_2, (with $a_2 \leq a_1$) and the corresponding vectors v_1 and v_2. Rules for identifying specific topographic features such as ridge, trench (inverted ridge), pit, saddle, plateau regions, are based on some combinations of the descriptor quantities.[5,6] Vessels, being darker than the background, appear as trenches and have been segmented using the curvature descriptor.[7] The Eigen vectors v_2 at neighbouring points in a trench are oriented in the same direction, provided the trench does not bend or branch at any of these points. This observation is used to detect the vessel junction and crossover points. Consider a neighborhood N_p around a point p in I_g. Let h_p be the curvature orientation histogram (COH) of the directions of v_2 of points in N_p.We define a dispersion measure $E(p)$ based on the entropy in h_p to determine the saliency of p and local maximas of $E(p)$ are declared as landmarks.

2.1 Pre-processing

In a flat region, the curvature magnitudes are negligible, and $v_2 \approx \vec{0}$. Flat regions do not yield points of high information content, and hence we restrict the computation of H at only image discontinuities, specifically vessel pixels. Since extraction of all junction points is not necessary, a simple method suffices to extract vessel pixels. A background estimation[8] by median filtering I_g is performed and suppressed from I_g by subtraction, to obtain a shade corrected image I_{sc}. Blood vessels are extracted based on the fact that they have negative

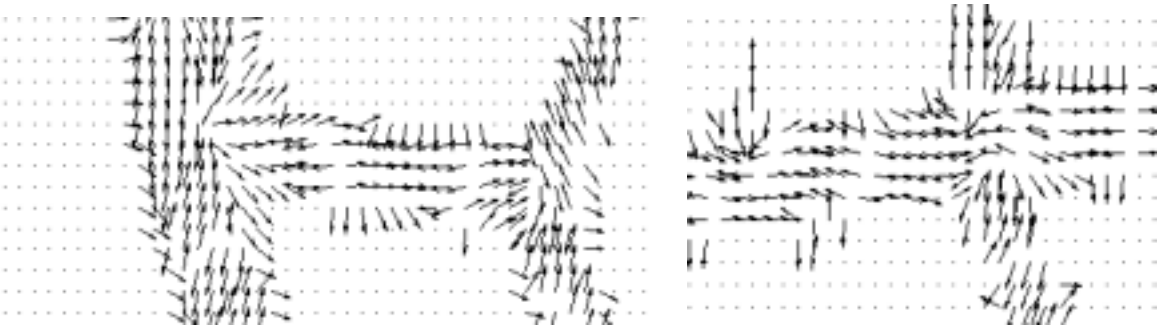

(a) (b)

Figure 1. Direction of v_2 on and around vessel pixels

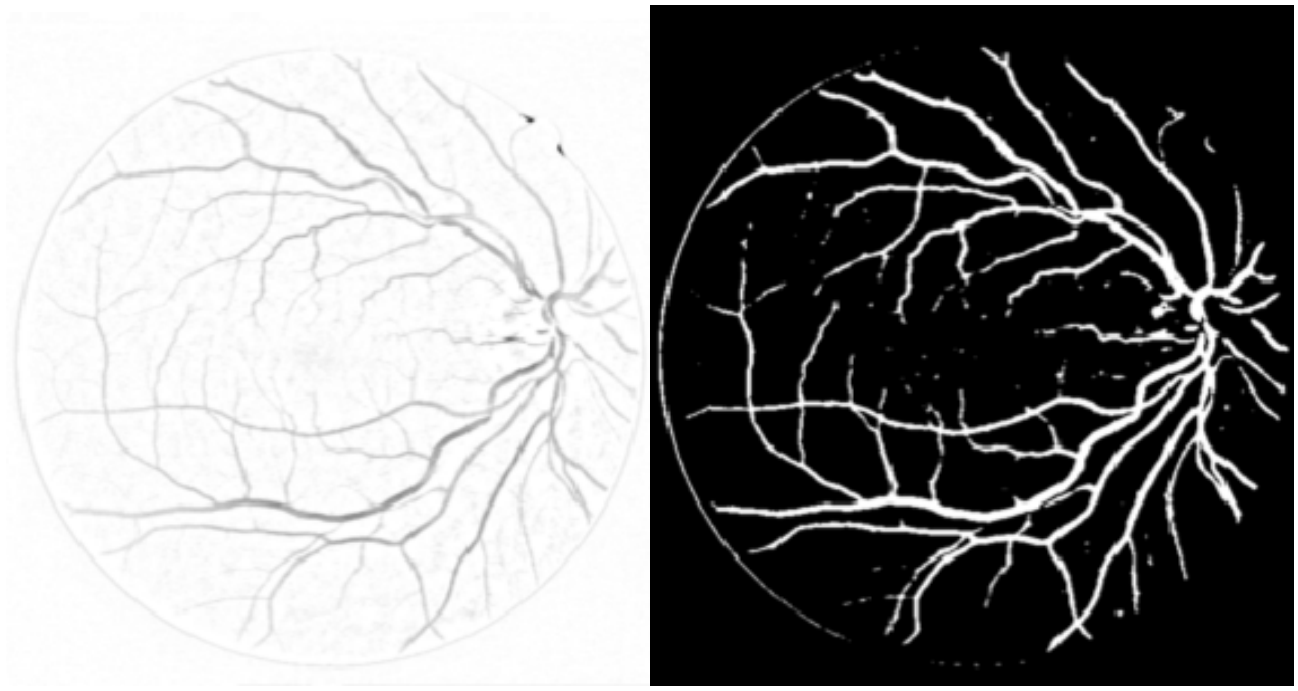

(a) Pre-processed image I_{pp} (b) Vessel map I_v obtained by thresholding I_{pp}

Figure 2. Pre-processing for obtaining a vessel map

values in I_{sc}. They are then shifted to positive values by adding $|\min(I_{sc})|$ to get pre-processed image I_{pp}. The background has uniform high value in I_{pp}, while vessels and dark regions occupy lower intensity levels. Since, majority($\approx 90\%$) of the pixels are in the background region a binary vessel map is obtained via simple thresholding. Next, a morphological thinning followed by closing is applied to retain only the pixels on and around the medial axis of vessels. This vessel map is denoted as I_v.

2.2 Dispersion measure

For every vessel pixel p in I_v, we compute orientation vectors v_2 from I_g and then the COH h_p, by considering a neighborhood N_p on I_v. The dispersion measure E which is the entropy of this COH is found as

$$E(p) = \sum_{i=1}^{n} h_p(i) \log \frac{1}{h_p(i)}. \quad (1)$$

Thus, corresponding to the vessel map I_v, we now have a dispersion map E. Note that at any point p the value of $E(p)$ will be high when the orientations of v_2 within N_p do not align, signifying the presence of a junction at p, while $E(p)$ will be low in the absence of a junction as the orientations of v_2 directions are roughly along the progression of the vessel. We obtain landmarks $P = \{\hat{p}\}$ from E by applying non-maximum suppression. The complete algorithm for landmark detection is given over-leaf.

2.3 Landmark Detection Results

Images from the STARE[9] and DRIVE[10] dataset have been used to test our approach. The Hessian matrix was computed at the vessel pixels on I_g using Gaussian smoothing with a 9×9 mask ($\sigma = 1$), and 3×3 Prewitt mask. The Eigen vector v_2 was normalized and a 5×5 neighborhood (N_p) was considered for obtaining a 12-bin orientation histogram h_p (angular resolution of 15^o). The entropy map E is computed and non-maximum suppression of E is performed, with radius 12 and threshold $th = \max(E)/2$, to obtain the landmarks.

algorithm $DETECT\_LANDMARKS(I)$

for each pixel p of I being identified as a vessel pixel **do**
  $H_p \leftarrow$ *Hessian matrix at* p
  $v_2 \leftarrow$ *second principal component of* H_p
  for each pixel q in $Neighbors(p)$ **do**
    $\theta_q \leftarrow \arctan(v_2y/v_2x)_q$
    $bin_q \leftarrow quantize(\theta_q, |B| + 1)$
    $B(bin_q) \leftarrow B(bin_q) + 1$
  end for
  $h_\theta(p) \leftarrow Entropy(B)$
end for
for each vessel pixel p **do**
  if $h_\theta(p) > \beta$ **then**
    $L \leftarrow L \cup p$
  end if
end for

A sample result of applying landmark detection in an image from the STARE dataset is shown in Fig. 3. The algorithm is able to detect junctions in the pigmented periphery of the image, as well as in the region near the optic disk which is more uniform. The right angles of the mask notch show similar characteristics in curvature change as a junction, and are hence falsely detected.

More sample results of detected landmarks using our method is shown in Figs. 4, 5(a), 5(b). The method

Figure 3. Landmarks detected on a STARE image

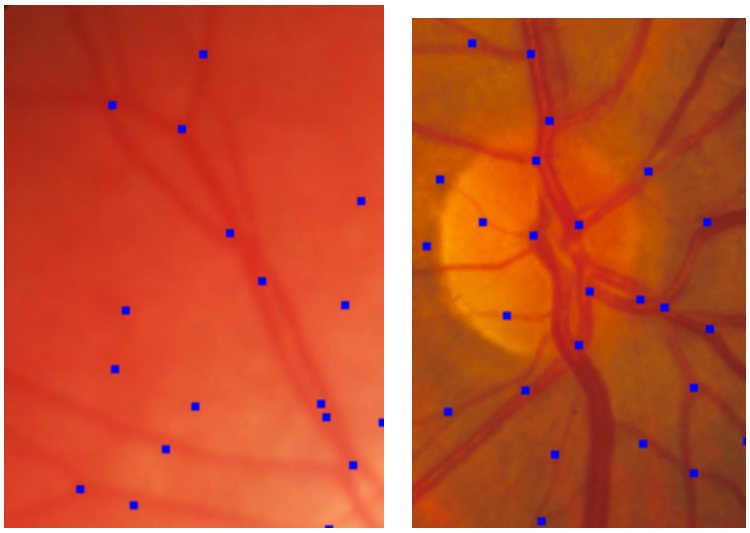

(a) Detections on a blurred image (b) Detections near optic disk

Figure 4. Results of landmark detection in different local contexts

is capable of detecting landmarks in regions of high blur in the image, as seen in Fig. 4(a), but some false positives arise, which could be attributed to small bumps on vessels or the capillary network. Fig. 4(b) shows the detections near the optic disk of an image. These results show that the algorithm is reasonably robust to changing context and can handle blur.

The quality of a retinal image is often non-uniform within an image. This will affect the landmark detection since the vessel detection is essential for good landmark detection. This can be seen from the result obtained in a low contrast region in Fig. 5(a). A solution to increasing the number of detected junctions is to improve the contrast of vessels prior to the detection step. For instance, applying retinex method[11] to enhance the retinal image improves the accuracy of localization of landmarks as seen in Fig. 5(b).

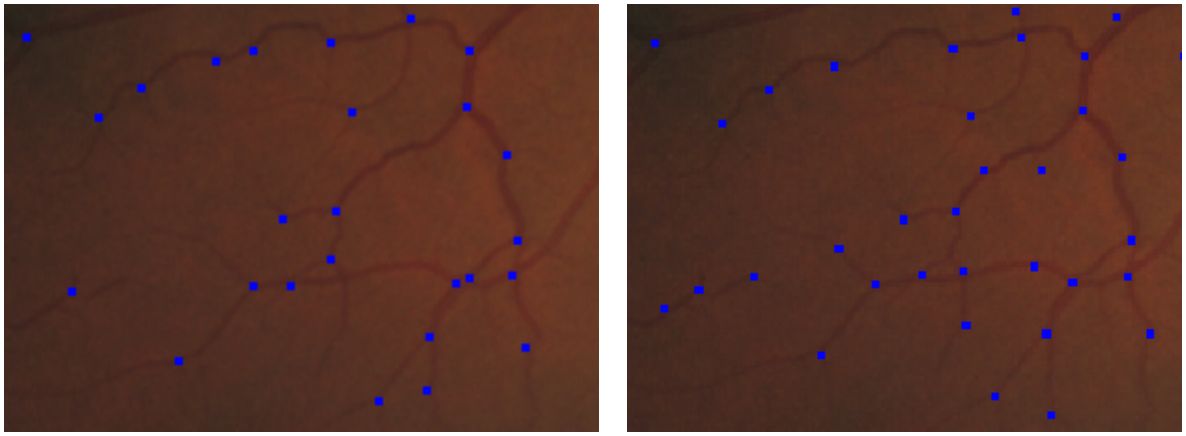

(a) Landmarks in low-contrast region of a STARE image (b) Improved localization with retinex enhancement

Figure 5. Landmark detection results

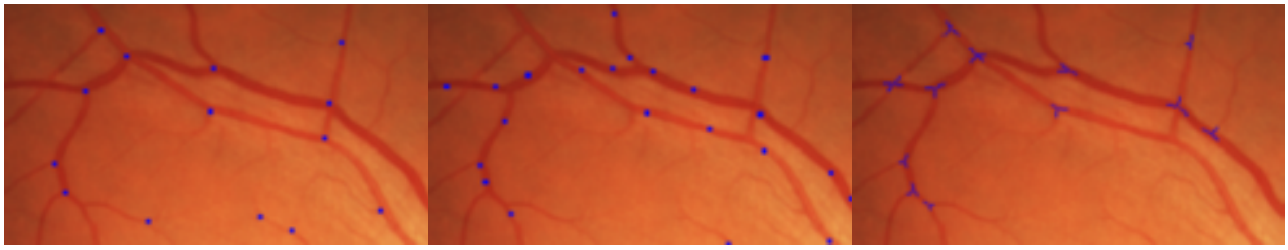

(a) Our method (b) Gradient-vector based method[2] (c) Vessel tracing based method[4]

Figure 6. Comparison of different approaches to landmark detection

To assess the performance of the proposed method against existing ones, two methods were chosen: one which used a dispersion measure on gradient vectors[2] and another which uses vessel tracing.[4] * Sample results on a sub-image are shown in Figs. 6(a), 6(b) and Fig. 6(c) respectively.

Results indicate that the gradient-based method produces denser set of landmarks compared to the proposed method. However, they occur anywhere along the vessel and not necessarily at the junctions. The vessel tracing-based method on the other hand yields fewer landmarks and similar to the proposed method, only if the vessels are detected. Branch points on some minor vessels and a T-shaped branch are not detected in Fig. 6(c), because the incident vessels were not detected. Likewise junctions with a faintly visible branch are missed by the proposed method. Obtained results show that the proposed method provides landmarks that are sparser and maximally informative as they coincide with junctions.

2.4 Correspondence computation scheme

We now show a way to use COHs to find the correspondence between two sets of landmark points. Apart from being the basis of the landmark detection step, the COHs encode descriptive information about the landmarks. The curvature orientation measures changes in the landmark's local neighborhood. Consequently the histogram of their orientations is a translation and rotation-invariant representation, which we use for matching.

Sample sub-images related by rotation and the corresponding COH pairs are shown in Fig. 7. The histograms are similar in the number and organization of the peaks, and can be roughly related by a cyclic shift. We have devised a method to capture the degree of similarity between shifted histograms, which yields a cumulative cost for each set of putative matches (called correspondence set C_i).

Let $P_1 = \{\hat{p}_1\}$ and $P_2 = \{\hat{p}_2\}$ be the set of landmark points computed from two images I_1 and I_2 related by a rigid transformation. Let $\Phi_1 = \{h_{1i}, 1 \leq i \leq m\}$ and $\Phi_2 = \{h_{2j}, 1 \leq j \leq n\}$, $m \leq n$ be the respective set of COHs. We compute a $m \times n$ distance matrix D^0 between the histograms in Φ_1 and Φ_2, where D^0_{ij} is the distance between h_{1i} and h_{2j} using an appropriate histogram distance measure. Smaller values of D^0_{ij} signify a good match between P_{1i} and P_{2j}.

For each $1 \leq i \leq m$, we find $\hat{j}$ for which $D^0_{i\hat{j}}$ is minimum. We then check if $D^0_{\alpha\hat{j}}$ is minimum at $\alpha = i$ for all $1 \leq \alpha \leq m$, to add the tuple (P_{1i}, P_{2j}) to the initial correspondence set C^0. Different correspondence sets C^k are obtained by applying circular shifts to COHs in Φ_2 and recomputing the new distance matrix D^k, k denoting the shift size. A cost function λ_k is computed for each C^k as follows.

$$\lambda_k = \frac{1}{|C^k|} \sum_{(i,j) \in C^k} D^k_{ij} \tag{2}$$

The best correspondence set is found as C^b where $b = \arg\min_k \lambda_k$.

A sample result of testing the above scheme using a rotation of 16^o is shown in Fig. 8. The earth mover's distance[12] was used to compute D^k and ground distances were provided considering the cyclic nature of the

*Fig. 6(c) was generated using executable provided in http://www.cs.rpi.edu/šofka/vessels.html

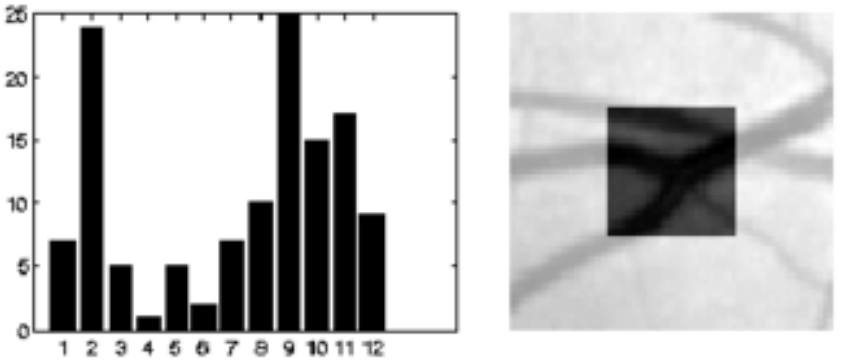

(a)

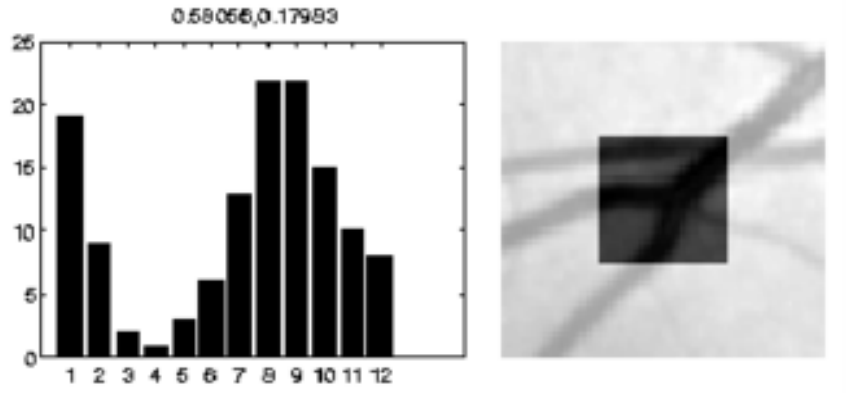

(b)

Figure 7. COH at a junction before and after transformation

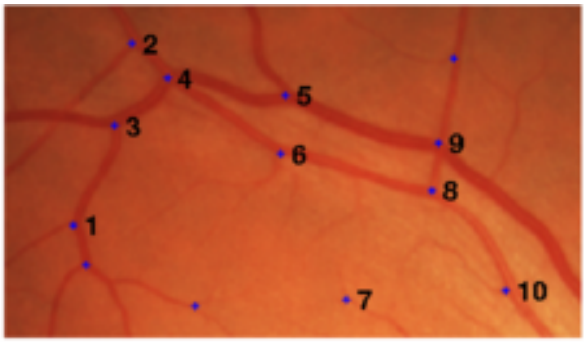

(a) Detections on a sub-image

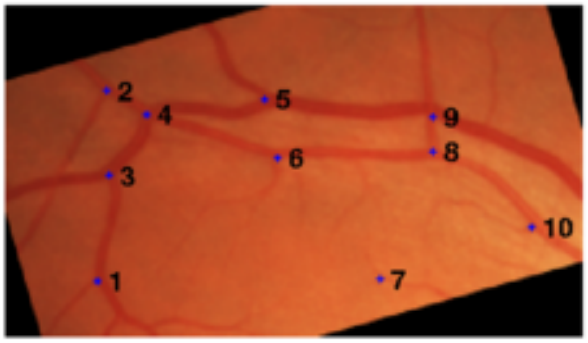

(b) Detections on sub-image rotated by 16^o

Figure 8. Corresponding landmarks between an image and its transformed version

k	0	1	2	3	4	5	6	7	8	9	10	11
λ_k	0.685	**0.242**	0.535	0.647	0.786	0.627	0.716	0.668	0.518	0.614	0.751	0.629
$\|C^k\|$	8	10	5	5	5	4	4	5	4	5	5	3
$\|w_k\|$	5	10	2	1	0	0	1	1	0	0	0	1

Table 1. λ_k values for our 12-bin histograms.$|w_k|$ denotes the number of matches visually found to be correct in C^k

orientation space. Table 1 shows the values of λ_k for 12 shifts of COHs computed over a 15×15 window. The match illustrated in Fig. 8 is obtained for $k = 1$ which indicates that the images are related by a rotation between 15 to 30 degrees.

From the above results, we see that the COH has potential to be used directly in correspondence computation. We have not considered scale variation, which requires parameterization of the COHs on scale (or neighborhood size). This is a significant consideration when the algorithm is extended to multi-modal matching.

3. CONCLUSION

A simple approach to detect retinal landmark points on vasculature has been proposed based on entropy of the COH computed in the neighborhood of a point. Our method provides a set of sparse, yet maximally informative set of landmarks (junctions). The attractive feature of the method is that the COHs implicitly capture the vessel branching information at a landmark point including the angles between them. In retinal images, this information remains invariant to rigid transformation. This is very useful in establishing correspondence between sets of landmark points obtained from images related by rigid transformations, as has been illustrated. However, in the real scenario, retinal images can undergo scale variation and shear as well. While the former can be handled by a scale space extension to COH analysis, the latter needs further investigation. Overall, the proposed landmark detection approach has potential for application in tracking of pathology.

REFERENCES

[1] Asada, H. and Brady, M., "The curvature primal sketch," *PAMI* **8**(1), 2–14 (1986).
[2] Becker, D., Turner, J., Tanenbaum, H., and Roysam, B., "Real-time image processing algorithms for an automated retinal laser surgery system," *ICIP* **1** (1995).
[3] Zana, F. and Klein, J., "A multi-modal registration algorithm of eye fundus images using vessels detection and hough transform," *IEEE Transactions on Medical Imaging* **18**(5) (1999).
[4] M.Sofka and C.V.Stewart, "Retinal vessel centerline extraction using multiscale matched filters, confidence and edge measures," *IEEE Transactions on Medical Imaging* **25**(12), 1531–1546 (2006).
[5] Haralick, R., Watson, L., and Laffey, T., "The topographic primal sketch," *International Journal of Robotics Research* **2**(1) (1983).
[6] Frangi, A. F., Niessen, W. J., Vincken, K. L., and Viergever, M. A., "Multiscale vessel enhancement filtering," *Lecture Notes in Computer Science* **1496** (1998).
[7] Garg, S., Sivaswamy, J., and Chandra, S., "Unsupervised curvature-based retinal vessel segmentation," *ISBI* , 344–347 (2007).
[8] Niemeijer, M., Ginneken, B. v., Staal, J., Suttorp-Schulten, M. S., and Abramoff, M. D., "Automatic detection of red lesions in digital color fundus photographs," *IEEE Transactions on Medical Imaging* **24**(5), 584–592 (2005).
[9] "Stare project website." http://www.ces.clemson.edu/ãhoover/stare.
[10] Staal, J., Abramoff, M., Niemeijer, M., Viergever, M., and van Ginneken, B., "Ridge based vessel segmentation in color images of the retina," *IEEE Transactions on Medical Imaging* **23**, 501–509 (2004).
[11] Frankle, J. A. and McCann, J. J., "Method and apparatus for lightness imaging." US Patent (1983).
[12] Rubner, Y., Tomasi, C., and Guibas, L., "A metric for distributions with applications to image databases," *ICCV* , 59–66 (1998).